# DEVELOPMENT AND CHARACTERIZATION OF TECHNETIUM-99M RADIOLABELED NANOPARTICLES

**AMIR FIRDAUS BIN ABDUL AZIZ**

**UNIVERSITI SAINS MALAYSIA**

**2023**

# DEVELOPMENT AND CHARACTERIZATION OF TECHNETIUM-99M RADIOLABELED NANOPARTICLES

**by**

**AMIR FIRDAUS BIN ABDUL AZIZ**

**Thesis submitted in fulfilment of the requirements**
**for the degree of**
**Master of Science**

**September 2023**

## ACKNOWLEDGEMENT

I thank Allah SWT for giving me the chance to complete this thesis entitled "Development and Characterization of Technetium-99m Radiolabeled Nanoparticles." The findings of this study are likely to inspire researchers working on nanoparticle-based SPECT radiotracers. My heartfelt thanks go to my primary supervisor, Dr. Amirah binti Mohd Gazzali, for all her help, advice, and direction in completing this study. I am very grateful to have a supervisor that is concerned and compassionate. A special thanks goes out to my field supervisor, Dr Fadzilah binti Hamzah, who provided me a lot of motivation to finish my thesis. In completing my research, I have collaborated with many parties including colleagues in the laboratory whom I respect, staff and lecturers at the School of Pharmaceutical Sciences, Universiti Sains Malaysia (USM) and staff at the Department of Nuclear Medicine, Penang Hospital. I would like to express my deepest gratitude to all parties involved either directly or indirectly in helping me with my work throughout this journey. For my wife and children, I am extremely pleased to have this family; they assist me and provide moral support in my attempts to accomplish this thesis. Without their encouragement and understanding it would be impossible for me to complete this work. To the Ministry of Health Malaysia, thank you very much for the financial support given to me throughout my studies at the School of Pharmaceutical Sciences, Universiti Sains Malaysia. Alhamdulillah.

**TABLE OF CONTENTS**

## LIST OF TABLES

**Page**

## LIST OF FIGURES

**Page**

## LIST OF SYMBOLS

| | |
|---|---|
| α | Alpha |
| Bq | Becquerels |
| β | Beta |
| $\beta^-$ | Beta minus |
| ɣ | Gamma |
| $t_{1/2}$ | Half-life |
| keV | Kilo electrovolts |
| MBq | Megabecquerel |
| μCi | Microcurie |
| μg | Microgram |
| mCi | Millicurie |
| mV | Millivolts |
| nm | Nanometer |
| $\beta^+$ | Positron |
| ζ | Zeta |

## LIST OF ABBREVIATIONS

| | |
|---|---|
| β-CD | Beta-cyclodextrin |
| $^{11}C$ | Carbon-11 |
| DTPA | Diethylenetriamine penta acetic acid |
| DMSA | Dimercapto succinic acid |
| EC | Electron capture |
| $^{18}F$ | Fluorine-18 |
| $^{67}Ga$ | Gallium-67 |
| $^{68}Ga$ | Gallium-68 |
| HMPAO | Hexamethylpropylene amine oxime |
| HDP | Hydroxydiphosphonate |
| $^{111}I$ | Indium-111 |
| $^{123}I$ | Iodine-123 |
| $^{124}I$ | Iodine-124 |
| $^{131}I$ | Iodine-131 |
| IT | Isomeric transition |
| MAG3 | Mercapto acetyl triglycine |
| $^{99m}Tc$ | Metastable Technetium-99 |
| MDP | Methylene diphosphonate |
| $^{99}Mo$ | Molybdenum-99 |
| $^{13}N$ | Nitrogen-13 |
| $^{15}O$ | Oxygen-15 |
| PET | Positron emission tomography |
| PET-CT | Positron emission tomography-computed tomography |
| SPECT | Single photon emission tomography |

| | |
|---|---|
| SPECT-CT | Single photon emission tomography-computed tomography |
| NaOH | Sodium hydroxide |
| TPP | Sodium tripolyphosphate |
| $SnCl_2$ | Stannous chloride |
| $^{201}Tl$ | Thallium-201 |
| TRODAT-1 | Tropane derivative (targeting dopamine transporter) |
| $^{89}Zr$ | Zirconium-89 |

## LIST OF APPENDICES

**PEMBANGUNAN DAN PENCIRIAN NANOPARTIKEL DIRADIOLABELKAN TECHNETIUM-99M**

## ABSTRAK

*Pengenalan*: Sifat fizikal technetium-99m ($^{99m}$Tc) yang menarik telah menjadikannya radionuklid yang lazim digunakan dalam pengimejan SPECT. Dalam bidang perubatan nuklear, potensi tinggi nanopartikel sebagai agen diagnostik apabila diradiolabelkan dengan $^{99m}$Tc telah menarik perhatian kebanyakan penyelidik. Kajian ini bertujuan untuk membangunkan dan mencirikan nanopartikel diradiolabelkan $^{99m}$Tc, daripada kitosan dan beta-siklodekstrin (β-CD). *Kaedah:* Nanopartikel kitosan telah disediakan menggunakan kaedah penggelan ionotropik dan kesan beberapa parameter terhadap saiz partikel dan kestabilan nanopartikel yang terbentuk, telah dinilai. Nanopartikel yang dioptimumkan kemudiannya diradiolabelkan dengan $^{99m}$Tc, dan kestabilan kompleks dinilai. Kesesuaian naopartikel β-CD untuk diradiolabelkan dengan $^{99m}$Tc juga dinilai dan dicirikan sewajarnya. *Keputusan:* Kepekatan optimum kitosan dan pH untuk menghasilkan nanopartikel kitosan masing-masing ialah 0.5 mg/ml dan pH 4.6, di mana saiz partikel terkecil yang diperoleh ialah 81 ±6.7 nm dengan taburan saiz sempit (PDI = 26 ±0.4%). Partikel menunjukkan kestabilan yang baik untuk sekurang-kurangnya 5 bulan. Nanopartikel β-CD sebaliknya mempunyai saiz partikel 692 ±40.7 nm dan saiz partikel kekal stabil untuk satu hari. Nanopartikel yang dihasilkan kemudiannya diradiolabelkan dengan $^{99m}$Tc, dengan julat aktiviti 100-111 MBq (2.7-3 mCi). Kecekapan pelabelan yang direkodkan adalah lebih daripada 90%, dengan kestabilan peradiolabelan lebih daripada 2 jam bagi β-CD, dan lebih 6 jam untuk nanopartikel kitosan. *Kesimpulan*: Berdasarkan penemuan, adalah mungkin

untuk membuat kesimpulan bahawa kedua-dua nanopartikel kitosan dan β-CD adalah sesuai untuk diradiolabelkan dengan $^{99m}$Tc.

# DEVELOPMENT AND CHARACTERIZATION OF TECHNETIUM-99M RADIOLABELED NANOPARTICLES

## ABSTRACT

*Introduction:* The appealing physical properties of technetium-99m ($^{99m}$Tc), have made it a commonly utilized radionuclide for SPECT imaging. In the field of nuclear medicine, the high potential of nanoparticles as a diagnostic agent when radiolabeled with $^{99m}$Tc has attracted the attention of many researchers. This study aims to develop and characterize $^{99m}$Tc-radiolabeled nanoparticles from chitosan and beta-cyclodextrin (β-CD). *Methods:* Chitosan nanoparticles were prepared using the ionotropic gelation method, and the effects of several parameters on the particle size and stability of the formed nanoparticles were evaluated. The optimized nanoparticles were then radiolabeled with $^{99m}$Tc, and the stability of the complex was evaluated. The suitability of β-CD nanoparticles for radiolabeling with $^{99m}$Tc was also evaluated and characterized accordingly. *Results*: The optimal concentration of chitosan and the pH for producing chitosan nanoparticles was 0.5 mg/ml and pH 4.6, respectively, and the smallest particle size obtained was 81 ±6.7 nm with a narrow size distribution (PDI = 26 ±0.4 %). The particles showed good stability for at least 5 months. β-CD nanoparticles on the other hand, has a particle size of 692 ±40.7 nm, and the particle size remains stable for one day. The produced nanoparticles were then radiolabeled with $^{99m}$Tc, with an activity range of 100–111 MBq (2.7–3 mCi). The labelling efficiency recorded was more than 90%, with a radiolabeling stability of 2 hours for β-CD and more than 6 hours for chitosan nanoparticles. *Conclusions*: Based on the findings, it is possible to conclude that both chitosan and β-CD nanoparticles are suitable for radiolabeling with $^{99m}$Tc.

# CHAPTER 1

# INTRODUCTION

## 1.1 Background

Nuclear medicine is a discipline of medicine that uses radionuclides in diagnostic and therapeutic procedures. The application of hybrid PET-CT scanner has enabled radiotracer localization, which has improved the detection sensitivity and specificity of certain diseases, including solid tumors (Vijayakumar et al., 2022). Although PET-CT scanners are the most advanced imaging machines in nuclear medicine, SPECT machines are still widely used (Xiao et al., 2022). One possible explanation for the widespread use of SPECT to this day is the readily available technetium-99m ($^{99m}$Tc), the most commonly used SPECT radiotracer in nuclear medicine.

As per the International Atomic Energy Agency (IAEA), "tracers" refer to substances possessing atomic or nuclear, physical, chemical, or biological properties that facilitate the identification, observation, or tracking of diverse physical, chemical, or biological processes. Radioisotopes are the examples of radioactive tracers, which are commonly known as radiotracers. Radiotracers utilised for diagnostic or therapeutic applications, such as imaging or radionuclide therapy, are commonly known as radiopharmaceuticals. This is due to the fact that they must conform to pharmaceutical standards for human use (Ruth, 2009).

The utilization of the gamma-emitting radioisotope $^{99m}$Tc is advantageous due to its short half-life of 6.02 hours and its accessibility through an economical radioisotope generator, costing approximately MYR 8,500 per generator and providing an activity of about 1000 mCi. This can benefit over 100 patients, depending on the type of scan conducted. In contrast, PET radiotracers mostly require production from a

cyclotron, costing around MYR 7,500 per vial of 200 mCi (at the doorsteps) and only benefiting 10 to 15 patients due to their shorter half-life ($^{18}$F-FDG, $t_{1/2}$ approximately 110 minutes; ~ 2 hours).

The free $^{99m}$Tc that is unattached to any targeting moiety has the tendency to accumulate in the thyroid gland, salivary gland, and gastric mucosa (Miftari et al., 2023). Hence, to improve its delivery towards specific organs, $^{99m}$Tc can be tagged with specific targeting moieties. The ability of nanoparticles to deliver drugs and/or radioactive materials to a particular target site is very promising. Numerous radiolabeled nanoparticles have been developed, and they are excellent radiotracers for a range of diagnostic applications (Felber and Alberto, 2015; Karageorgou et al., 2017; Salih et al., 2022).

Chitosan, which has several fascinating properties such as biocompatibility and biodegradability, has been the subject of countless scientific investigations to explore its potential in different applications, including artificial skin, bone regeneration, dental implants, surgical sutures, wound repair, and drug delivery. Chitosan can be produced by deacetylation of chitin, the second most abundant polysaccharide after cellulose. Chitin is available from various sources such as crustacean shells, insects, in the cell walls of fungal, algae and yeasts. Crabs and shrimps, however, were the primary sources of chitin used in industrial applications (Elieh-Ali-Komi et al., 2016; Pakizeh et al., 2021).

In recent years, there has been an increased in the number of researchers interested in chitosan nanoparticles as a suitable carrier for drug delivery. Numerous methods can be used to produce chitosan nanoparticles such as the emulsification/solvent evaporation method, the polyelectrolyte complexation method, the reverse micellar method/microemulsion method, and the ionotropic gelation

method. The first reported chitosan nanoparticles synthesis was by Ohya et al. (1994) which was conducted through the emulsification and cross-linking method (Tian et al., 2023).

## 1.2 Problem Statement

Most of the time, in a diagnostic nuclear medicine setting, radioisotopes such as $^{99m}$Tc are often used to detect a specific disease area or as an agent to evaluate the effectiveness of treatment. To facilitate the delivery of these radioisotopes to the intended location, they are commonly attached to targeting moieties. One instance is the use of a targeting agent known as methylene diphosphonate (MDP), which is accessible in diagnostic kit form in the clinical setting. This kit is radiolabeled with $^{99m}$Tc to form a $^{99m}$Tc-MDP complex used for bone imaging purposes. This radiolabeling process is done at the Radiopharmacy Unit at the Nuclear Medicine Department in tertiary hospitals prior to its administration to patients.

In recent years, nanoparticles have attracted the attention of researchers in their potential as theranostic agents. The term "theranostics" is used to describe the practice of combining diagnostic agents with therapeutic drugs that share a specific target in diagnosing and treating a disease. Nanoparticles offer several advantages including targeted delivery and enhanced permeability and retention effect. In addition, according to Daems et al. (2021), nanoparticles have the capacity to hold multiple radionuclides, resulting in significantly higher radioactivity payloads than a single or small number of radionuclides carried by a conventional radiopharmaceutical agent. This indirectly presents a possibility for the nanoparticles to potentially enhance the detection limit and resolution of imaging applications in an indirect manner. Radiopharmaceuticals are pharmaceutical compounds that have been labelled with radionuclides, commonly

known as radioactive drugs. These substances are utilized as a source of ionizing radiation for both diagnostic and therapeutic applications (Parrilha et al., 2022). With this advantage, nanoparticles that are radiolabeled with radionuclides are not only useful for imaging (diagnosis), but they are also very useful for therapy as well as theranostic agents, depending on the radionuclide used.

However, there are still several challenges that need to be addressed, including optimization of nanoparticles size, shape, and surface chemistry, besides ensuring sufficient radiolabeling capacity and the stability of the radiolabeled nanoparticles. This will be answered through this study and the finding will have important implications for the development of new and effective tumor diagnostic agent that can potentially contribute to the improvement of overall patient outcomes.

## 1.3 Research Aims and Objectives

The main aims of this study were to describe the development of chitosan nanoparticles and to characterize the resulting nanoparticles. β-CD nanoparticles will also be evaluated upon reconstitution. Both nanoparticles will then be radiolabeled with $^{99m}$Tc which could be potentially useful as SPECT imaging radiotracers.

### 1.3.1 Specific Objectives

a. To synthesize chitosan nanoparticles and characterize them in terms of particle size, polydispersity index, and surface charge.
b. To evaluate the effect of upscaling process on the characteristics of the chitosan nanoparticles produced.
c. To radiolabel chitosan nanoparticles and β-CD nanoparticles with $^{99m}$Tc and evaluate the radiolabeling efficiency and stability of both carriers.

### 1.3.2 Significance of the Study

Nuclear diagnostic imaging has become a powerful tool in both preclinical and clinical research as well as in diagnosing and therapy of many diseases. Although PET-CT imaging is one of the most sophisticated machines in nuclear medicine, the use of SPECT or SPECT-CT imaging is still widespread. This is because $^{99m}$Tc, a gamma-emitting radioisotope, is readily accessible from a low-cost generator, as opposed to the positron-emitting radioisotope for PET-CT imaging, which is generally produced by an expensive cyclotron. Lately, the potential of $^{99m}$Tc-based radiolabeled nanoparticles has attracted attention that has spurred investigation in the theranostic of numerous diseases, especially tumors. Chitosan and β-CD that have several attractive properties like biocompatibility, biodegradability, and low toxicity, have been the subject of various scientific investigations that demonstrate their use in a wide range of applications. These nanoparticles have the potential to accumulate in tumor tissue and subsequently become one of the agents in the SPECT imaging of tumors in humans.

# CHAPTER 2

# LITERATURE REVIEW

## 2.1 Nuclear Medicine

### 2.1.1 Introduction

Nuclear medicine is a type of medical specialty that utilizes radionuclides for diagnostic procedures, including the staging and restaging of diseases and monitoring of therapy responses (Goel et al., 2023). It is a non-invasive diagnostic method that is used to detect *in vivo* abnormalities (Boudousq et al., 2022; Polvoy et al., 2020). The most common nuclear medicine diagnostic imaging techniques are single photon emission computed tomography (SPECT) and positron emission tomography (PET).

Services related to nuclear medicine have been available in Malaysia for nearly 60 years (Suppiah, 2021). At present, there are only six government facilities under the Ministry of Health, Malaysia that provide nuclear medicine services (Figure 2.1), with most of the facilities offers SPECT imaging in their routine clinical diagnostics work. Kuala Lumpur Hospital was the first hospital in Malaysia to introduce nuclear medicine services in 1964 (Suppiah, 2021). The other five government facilities are the National Cancer Institute in Putrajaya; Penang General Hospital, located in the northern part of Malaysia; Sultanah Aminah Johor Bahru Hospital, in the southern part of Malaysia; Sarawak General Hospital; and Sabah Women and Children Hospital (*Hospital Wanita dan Kanak-kanak Sabah*), both in East Malaysia (Fakhrurazi et al., 2016).

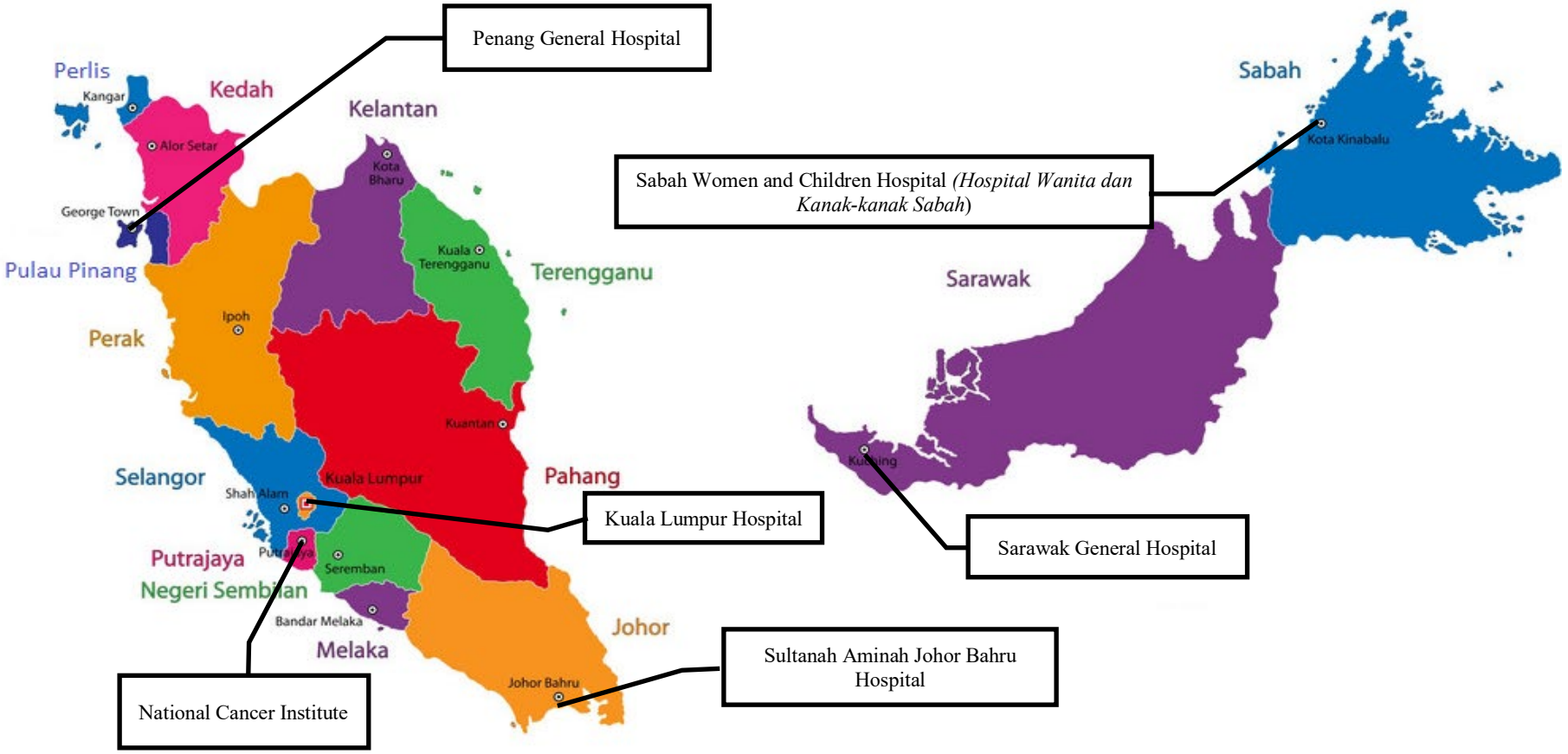


Figure 2.1 Nuclear medicine facilities at Malaysian government hospitals

### 2.1.2 Imaging Modalities

#### 2.1.2(a) Positron Emission Tomography (PET) and PET Radionuclides

PET is a functional imaging modality which can accurately measure *in vivo* distribution of a typically short-lived positron-emitting radionuclides or radiopharmaceutical, with a higher spatial resolution which enables better detection of smaller lesions (Kulshrestha et al., 2016; van der Vos et al., 2017). PET detects high-energy photon pairs emitted during positron decay of a radioisotope to produce high-resolution tomographic images (van der Vos et al., 2017).

The term "positron decay" in this context pertains to the process of "radioactive decay". Radioactive decay refers to the process in which an unstable atomic nucleus undergoes a loss of energy through the emission of radiation. Alpha- (α), beta- (β), and gamma- (ɣ) decay are among the most common types of decay, which involves the emission of one or more particles or photons. The emission of α-rays, or α-particles, occurs when an atom loses two protons and two neutrons from its nucleus in a process known as α-decay (Amanda Reichelt-Brushett and Joanne M. Oakes, 2023). Actinium-225 ($^{225}$Ac) is an example of alpha particle-emitter that has been widely used in radioimmunotherapy (Shalgunov et al., 2022). In β-decay, it involves the emission of β-particles. There are two types of β-decay: negative β-decay, and positive β-decay. In negative β-decay, the process involves the decay of a neutron located within the nucleus of an unstable atom, resulting in the production of a proton and an electron. The proton resulting from this decay remains in the nucleus, while the electron is emitted at high speed and is characterized as a negatively charged β-particle ($\beta^-$) (Amanda Reichelt-Brushett and Joanne M. Oakes, 2023). Iodine-131 is one of the examples of a radioisotope that undergoes beta-minus decay and is commonly used as a therapeutic agent in thyroid cancer (Sun et al., 2022). Meanwhile, in positive β-decay, instead of an

electron, a positively charged β-particle ($\beta^+$) is emitted during this process. This is due to the proton in the nucleus that decayed into a neutron, and the neutron remained in the nucleus. The $\beta^+$ particles, also known as positrons, are particles with comparable properties to electrons but a positive charge (Amanda Reichelt-Brushett and Joanne M. Oakes, 2023). Fluorine-18 and gallium-68 are examples of positron emitters that are commonly used as PET radiotracers (De Feo et al., 2023). ɣ-decay refers to the process by which a nucleus transitions from a higher energy state to a lower energy state, resulting in the release of excess energy in the form of high-energy photons, or electromagnetic radiation (Amanda Reichelt-Brushett and Joanne M. Oakes, 2023). Gallium-67, technetium-99m, indium-111 are the examples of gamma emitters that used in SPECT imaging (Salmanoglu et al., 2018).

However, PET alone is unable to provide anatomic localization of diseases, and instead, CT (Computed Tomography) could overcome the problem by providing detailed information about the structure and anatomy of the organ. Thus, with the development of a hybrid PET-CT scanner (Figure 2.2), localization of the tracer activity can be enhanced, and the sensitivity and specificity of disease detection can be improved (Vijayakumar et al., 2022).

Figure 2.2 Positron emission tomography-computed tomography (PET-CT) machine

PET-CT has emerged as a prominent imaging modality for diagnosing many diseases, including staging, restaging, and monitoring of therapy response for a wide range of malignancies (Araz et al., 2015). Positron-emitting radionuclides such as Zirconium-89 ($^{89}$Zr, $t_{1/2:}$ 3.3 days), Iodine-124 ($^{124}$I, $t_{1/2:}$ 4.2 days), Carbon-11 ($^{11}$C, $t_{1/2:}$ 20.4 min), Fluorine-18 ($^{18}$F, $t_{1/2:}$ 109.8 min), and Gallium-68 ($^{68}$Ga, $t_{1/2:}$ 67.7 min) are among the radionuclides used in PET imaging (Chakravarty and Chakraborty, 2021; Vranješ-Đurić and Ignjatović, 2018).

### 2.1.2(b) Single Photon Emission Computed Tomography (SPECT) and SPECT Radionuclides

Even though PET imaging can be considered as the most sophisticated imaging technique in nuclear diagnostic, it is fascinating to note that, Single Photon Emission Computed Tomography (SPECT) imaging is still in widespread usage today (Xiao et al., 2022). Since Kuhl and Edwards first demonstrated SPECT in the early 1960‘s, the technology has seen significant advancement (Varga et al., 2023). The difficulty of

acquiring anatomical localization with SPECT alone was overcome with the presence of a hybrid SPECT-CT (Figure 2.3) scanner which has improved the localization of tracer activity and the sensitivity and specificity of disease detection (Gonca G. Bural et al., 2012; Kaewput and Vinjamuri, 2022).

Figure 2.3 Single photon emission computed tomography-computed tomography (SPECT-CT).

Unlike PET imaging which employs positron-emitting radioisotopes, SPECT imaging uses gamma-emitters such as technetium-99m ($^{99m}$Tc) and indium-111 ($^{111}$I) **(**Table 2.1**)**. Gamma-rays that are emitted from a radiotracer or radiopharmaceutical, which are typically administered intravenously to the patient, are captured by one or more gamma camera heads that is rotated about the patient. SPECT images are cross-sectional slices that can be reconstructed into 3-dimensional images, and the combination with CT in the imaging process will improve the accuracy of anatomical localization of functional abnormalities, which aid in the diagnosis and monitoring of diseases (Tabotta et al., 2019; Yitbarek and Dagnaw, 2022). Technetium-99m ($^{99m}$Tc, $t_{1/2:}$ 6.02 hours) is the gamma-emitting radioisotope that is most often used in

SPECT/SPECT-CT imaging because it possesses excellent imaging characteristics. From a survey conducted by Fakhrurazi et al. (2016), $^{99m}$Tc was reported as one of the most widely used radioisotopes in Malaysia.

Table 2.1 Commonly used SPECT and PET radionuclides

**A. SPECT Radionuclides**

| Radionuclide | Physical Characteristics | | | Production Mode | References |
|---|---|---|---|---|---|
| | Half-life | Decay Mode | *E*(keV) | | |
| Technetium-99m ($^{99m}$Tc) | 6.02h | γ, IT | 140.5, 142.6 | Generator | (Crișan et al., 2022) |
| Indium-111 ($^{111}$I) | 67.2h (2.8d) | γ, EC | 173, 247 | Cyclotron | (Pandit-Taskar et al., 2015) |
| Gallium-67 ($^{67}$Ga) | 78.3h (3.26d) | γ, EC | 93, 184, 300 | Cyclotron | (Bailey et al., 2021) |
| Iodine-123 ($^{123}$I) | 13.2h | γ, EC | 159 | Cyclotron | (Morphis et al., 2021) |
| Iodine-131 ($^{131}$I) | 192.5h (8.04d) | $\beta^-$, γ | 364.5, 636.9 | Reactor | (Morphis et al., 2021; Yeong et al., 2014) |
| Thallium-201 ($^{201}$Tl) | 73.5h (3.06d) | γ, EC | 137, 167 | Cyclotron | (Malhotra et al., 2019) |

**B. PET Radionuclides**

| Radionuclide | Physical Characteristics | | | Production Mode | References |
|---|---|---|---|---|---|
| | Half-life | Decay Mode (%) | *Emax*(keV) | | |
| Carbon-11 ($^{11}$C) | 20.4 min | $\beta^+$(99.79), EC (0.21) | 960 | Cyclotron | (Crișan et al., 2022; Taddei and Pike, 2019) |
| Fluorine-18 ($^{18}$F) | 109.8 min | $\beta^+$(97), EC (3) | 634 | Cyclotron | (Chakravarty and Chakraborty, 2021; Cole et al., 2014; Kuker et al., 2017) |
| Gallium-68 ($^{68}$Ga) | 67.7 min | $\beta^+$(89), EC (11) | 1899 | Cyclotron/ Generator | (Bailey et al., 2021; Spang et al., 2016) |
| Iodine-124 ($^{124}$I) | 4.2 d | $\beta^+$(25.6), EC (74.4) | 2138 | Cyclotron | (Chakravarty and Chakraborty, 2021; Kuker et al., 2017) |
| Nitrogen-13 ($^{13}$N) | 9.96 min | $\beta^+$ | 1190 | Cyclotron | (Jochumsen et al., 2023) |
| Oxygen-15 ($^{15}$O) | 2.03 min | $\beta^+$ | 1740 | Cyclotron | (Jochumsen et al., 2023) |
| Zirconium-89 ($^{89}$Zr) | 78.41 h (3.3d) | $\beta^+$(22.3), EC (76.6) | 897 | Cyclotron | (O'Hara et al., 2022) |

IT = isomeric transition, EC = electron capture, $\beta^+$ = positron emission, $\beta^-$ = beta minus decay

## 2.2 Technetium-99m

### 2.2.1 Background

In contrast to radiotracers used in PET imaging that are typically produced by a cyclotron, the intriguing aspect of employing $^{99m}$Tc is that it can be easily obtained from a generator system. The shorter-lived daughter radionuclide $^{99m}$Tc can be eluted from the relatively long-lived parent radionuclide molybdenum-99 ($^{99}$Mo) via an inexpensive on-site $^{99}$Mo/$^{99m}$Tc generator system. This generator system has been available in nuclear medicine for more than 60 years since its first introduction by the Brookhaven National Laboratory in 1958 (Anderson et al., 2019). The relatively longer $t_{1/2}$ of $^{99}$Mo is an added advantage; its $t_{1/2}$ of about 66 hours (~ 3 days) means that there is an ample time for transportation of the $^{99}$Mo/$^{99m}$Tc generators from manufacturers to users, without the need for higher activity if the $t_{1/2}$ of the radioisotope is relatively short.

The decay of $^{99}$Mo proceeds through β-decay (Figure 2.4), and approximately 88% of these decays would lead to the production of the metastable technetium-99 ($^{99m}$Tc). $^{99m}$Tc is a pure gamma emitter that undergoes a process known as isomeric transition (Figure 2.4). During this process, $^{99m}$Tc decays to $^{99}$Tc with the release of gamma rays. About 98.6% of the decay emits 140.5 keV gamma rays and the remaining 1.4% emits 142.6 keV (Crișan et al., 2022). The low energy gamma photon that is emitted by $^{99m}$Tc, which is about 140 keV, is an ideal characteristic for imaging with gamma cameras (Park and Lee, 2023). In addition, with the physical $t_{1/2}$ of about 6 hours, it provides enough time for the preparation, administration, and distribution of the $^{99m}$Tc as well as for the diagnostic imaging to be conducted on patients.

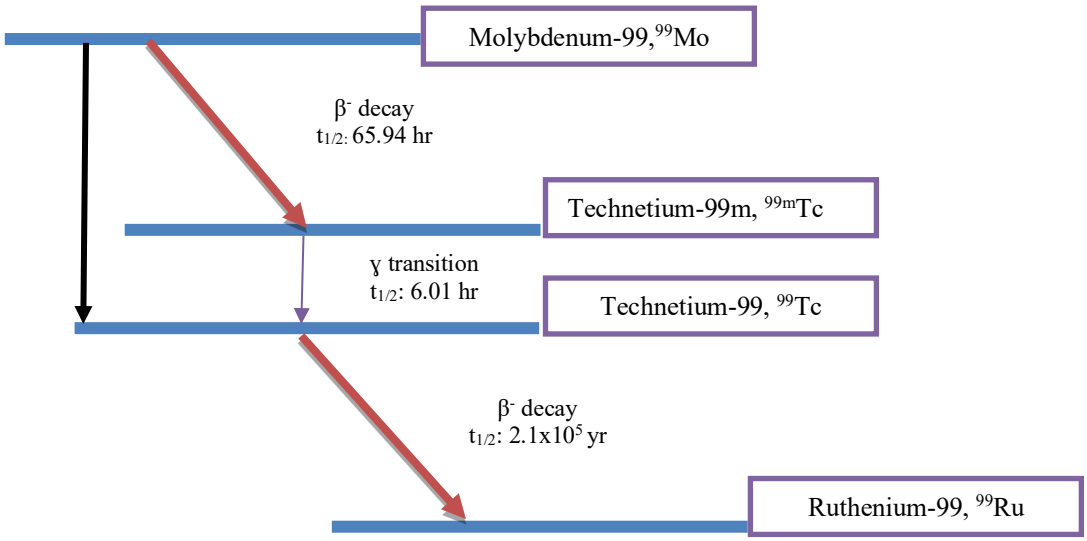


Figure 2.4 $^{99}$Mo and $^{99m}$Tc decay schemes

### 2.2.2 Types of $^{99}$Mo/$^{99m}$Tc Generator

Basically, there are two types of $^{99}$Mo/$^{99m}$Tc generator systems (Figure 2.5) that are commercially available, which are (1) dry-column generator and (2) wet-column generator. The dry-column system will have two ports, usually at the top of the generator: one for elution with sterile 0.9% sodium chloride solution (also known as normal saline or isotonic saline), and the other for the collection of $^{99m}$Tc with sterile evacuated vial. Meanwhile, the wet-column system, has a normal saline reservoir inside the generator itself, and the eluate is collected at a collecting port in a sterile evacuated vial. The term "dry-column" is referred to the column inside the generator that does not contain saline prior to the elution process; thus, it is called a "dry-column". For "wet-column" generator system, however, the column inside the generator is kept wet with saline. There are also generators that come with a dry column but function as a wet column after the first elution (Hung et al., 2000).

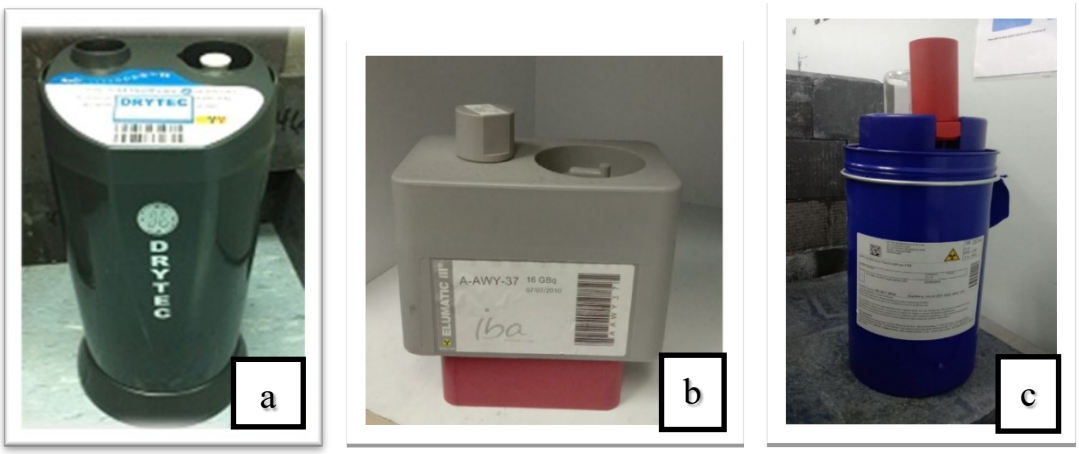


Figure 2.5 Examples of $^{99}Mo/^{99m}Tc$ generator: a) Dry-column generator, b) wet-column generator, and c) generator that come with a dry-column but function as a wet-column after the first elution

### 2.2.2(a) Elution of the Generator

The elution of $^{99m}Tc$ is conducted using a technique called column chromatography. This can be done repeatedly from the $^{99}Mo/^{99m}Tc$ generator system. In this system, $^{99}Mo$ in the form of molybdate ($MoO_4^{2-}$), is embedded in a column of alumina (aluminium oxide, $Al_2O_3$) which acts as an adsorbent. When $^{99}Mo$ decays, it produces pertechnetate, $TcO_4^-$, which has a lower affinity for the alumina than its parent radionuclide. $TcO_4^-$ then can be flushed out from the column by using an isotonic saline solution in the form of sodium pertechnetate. At certain concentrations, sodium pertechnetate can then be labelled with specific pharmaceuticals in accordance with the targeted organ or the type of scintigraphy to be performed (Table 2.2). These pharmaceuticals are usually commercially available in the form of ready-to-use kits (Chang et al., 2023).

Table 2.2 Several $^{99m}$Tc-based radiopharmaceuticals and their applications

| Radiopharmaceutical | Imaging | References |
|---|---|---|
| $^{99m}$Tc-DTPA | Kidney / Brain | (Gilad et al., 2012; Pi et al., 2023) |
| $^{99m}$Tc-DMSA | Kidney | (Lin et al., 2023) |
| $^{99m}$Tc-MAG3 | Kidney | (Weaver et al., 2023) |
| $^{99m}$Tc-MDP | Bone | (Jain et al., 2023) |
| $^{99m}$Tc-HDP | Bone | (Drissa et al., 2023) |
| $^{99m}$Tc-Sestamibi | Cardiac/Parathyroid/Breast | (Smith et al., 2023; Verrecchia-Ramos et al., 2023; Wang et al., 2023) |
| $^{99m}$Tc-Tetrofosmin | Cardiac/Parathyroid | (Alkhybari et al., 2023; Lalonde et al., 2023) |
| $^{99m}$Tc-Mebrofenin | Hepatobiliary | (Werner et al., 2023) |
| $^{99m}$Tc-HMPAO | Brain | (Zuckier and McKinnon, 2023) |
| $^{99m}$Tc-TRODAT-1 | Parkinson disease: Dopamine transporter | (Chang et al., 2023) |

### 2.2.2(b) Routine Test on the Eluate

Before the beginning of a radiolabeling procedure, the $^{99m}$Tc obtained from the generator was tested to ensure that the presence of impurities was within acceptable limits. There are two types of impurities that may be present with $^{99m}$Tc during the elution process: radionuclidic impurity and chemical impurity (Abedi et al., 2014; Hasan and Prelas, 2020). The molybdenum breakthrough test and the aluminum breakthrough test are two of the tests commonly carried out (Abedi et al., 2014; Hasan and Prelas, 2020). These are the standard tests performed prior to the preparation of any radiopharmaceutical. As discussed above, $^{99}$Mo has a strong affinity for alumina (aluminum oxide, $Al_2O_3$); yet, when saline was used to flush out $^{99m}$Tc from the generator to the sterile evacuated vials (collection vial), trace quantities of $^{99}$Mo may also be present in the vials. The presence of molybdenum in the evacuated vial is referred to as "molybdenum breakthrough", which is the major source of radionuclidic impurity in $^{99m}$Tc-based radiopharmaceuticals. According to the US Pharmacopeia, the presence of $^{99}$Mo in every 1 mCi of $^{99m}$Tc shall not exceed 0.15 μCi. Figure 2.6 shows the procedure carried out for the molybdenum breakthrough test.

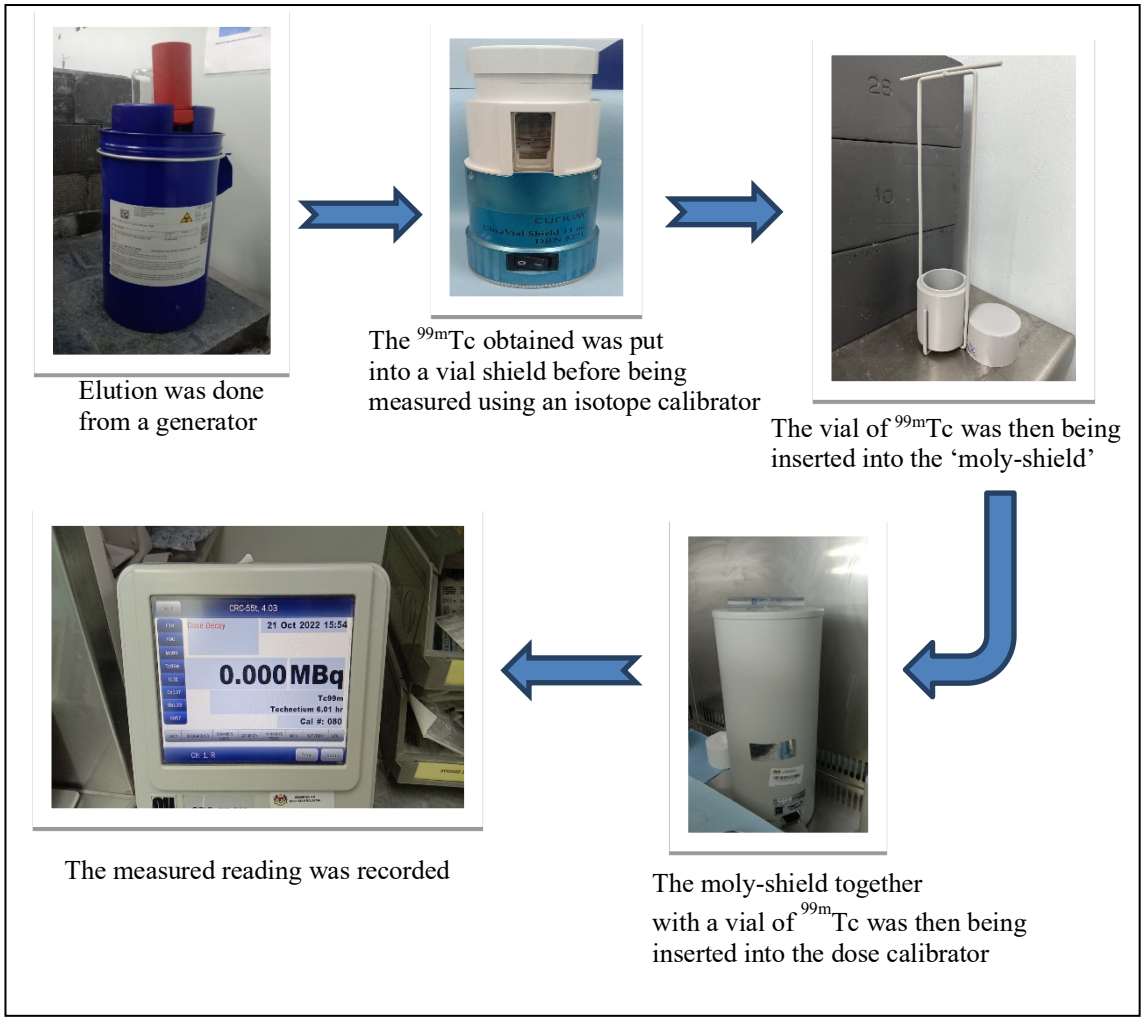


Figure 2.6 Molybdenum breakthrough test procedure

Another essential test that must be performed is the aluminum breakthrough test. The purpose of this test is to determine that the amount of aluminum ("aluminum breakthrough") present in the evacuated vial is within the allowed concentration, which is not more than 10 µg/mL as defined by the US Pharmacopeia. As illustrated in Figure 2.7, the aluminum breakthrough test is carried out through color intensity comparison; a drop of standard aluminum solution (10 µg/ml) is placed on one side of the indicator paper, and on the other side, a drop of $^{99m}$Tc is placed. The color intensity of the two droplets is then compared. If the drop of $^{99m}$Tc is redder than the aluminum standard

solution, this means that the presence of aluminum in the evacuated vial is above the acceptable limit (10 µg/ml) (Abedi et al., 2014; Hasan and Prelas, 2020).

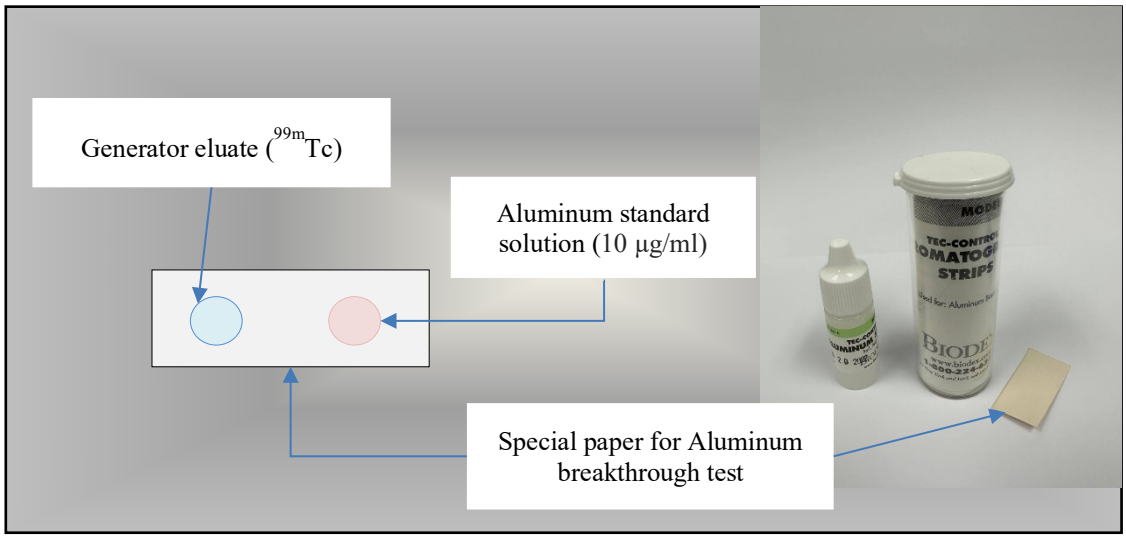


Figure 2.7 Aluminum breakthrough test

### 2.2.3 $^{99m}$Tc Radiolabeled Nanoparticles

As previously stated, radiotracers may be used to identify a specific disease area or as an agent to evaluate the efficacy of a therapy. Depending on the imaging procedure to be performed, $^{99m}$Tc can accumulate in specific organs in the presence of a suitable pharmaceutical that acts as a targeting agent. In the absence of targeting agents, the free $^{99m}$Tc in the form of pertechnetate ($^{99m}TcO_4^-$), will accumulate in the thyroid and salivary glands as well as gastric mucosa (Han et al., 2022). Recently, nanoparticles are increasingly attracting the interest of many researchers due to their uniqueness and advantages.

According to Daems et al. (2021), nanoparticles have the capacity to hold multiple radionuclides, which may result in a significantly higher radioactivity payloads than a single or limited number of radionuclides carried by a conventional radiopharmaceutical agent (Figure 2.8). With this advantage, nanoparticles that are radiolabeled with radionuclides are not only useful for imaging (diagnosis), but they are

also very useful for therapy as well as theranostic. In terms of drug delivery system, nanoparticles have great potential to deliver drugs or/and radionuclides to a specific target site of action. A variety of radiolabeled nanoparticles have been developed as useful radiotracers (Ahmadi et al., 2023; Felber and Alberto, 2015; Karageorgou et al., 2017; Mushtaq et al., 2021).

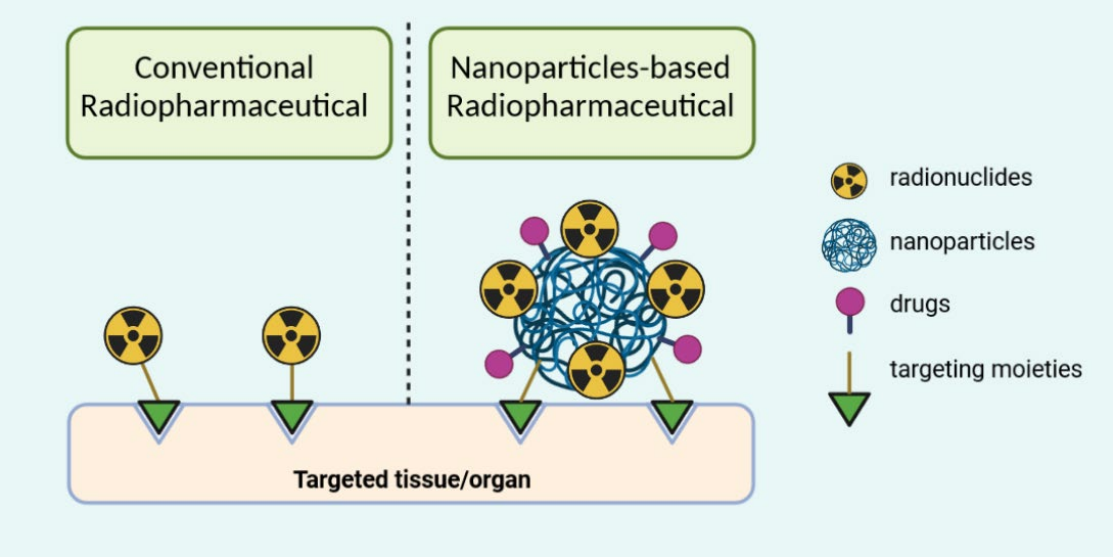


Figure 2.8 Comparison between conventional radiopharmaceutical and nanoparticles-based radiopharmaceutical

Nanoparticles can be defined as particles that have a size range between 1 and 1000 nm (Gundogdu et al., 2015; Jeevanandam et al., 2018; Ko et al., 2022). The small size of nanoparticles means they have a high surface area to volume ratio. The size range of nanoparticles could be tailored depending on the intended applications and this is important as particle size is known to have a significant impact on the biodistribution of nanoparticles. Particle sizes less than 100 nm have been shown to be biodistributed widely throughout several tissues or organs such as blood (De Jong et al., 2008), lungs (De Jong et al., 2008), and brain (Schroeder et al., 2012). Smaller particles of less than 5 nm, however, will be rapidly cleared *via* renal excretion (Pratt et al., 2016).

Based on available literatures, large particles will be rapidly detected and trapped by reticuloendothelial systems (RES) which are mainly located in the liver and spleen (Blanco et al., 2015; Haute and Berlin, 2017; Mitchell et al., 2021; Skotland et al., 2022). According to Colino et al., (2020), larger nanoparticles exhibit greater efficacy in terms of hepatic uptake, where a diameter greater than 200 nanometers is deemed preferable for deposition in the liver. The affinity of large nanoparticles for the mononuclear phagocyte system (MPS) can be benefited to facilitate the delivery of therapeutic agents to these cells by polymeric nanoparticles.

In a study conducted by Verdun et al. (1990), doxorubicin that are incorporated into polyisohexylcyanoacrylate (PIHCA) nanoparticles (average size 260 ±15 nm) exhibit high uptake in the liver. This biodistribution can aid the chemotherapeutic treatment of MPS-localized tumors, like hepatocarcinoma or hepatic metastasis (Snehalatha et al., 2008).

In order to avoid RES trapping, nanoparticles need to be within the optimal size range which is approximately between 100–200 nm (Wu, 2021). This will also indirectly facilitate the enhanced permeability and retention (EPR) effect in solid tumors, which means the nanoparticles will have a higher tendency to accumulate in tumor tissues as through passive tumors targeting compared to the normal tissues (Nakamura et al., 2016).

Meanwhile, Polyák et al. (2013) conducted a study utilizing active tumor targeting to achieve nanoparticles targeting. The investigation involves the radiolabeling of chitosan and folate poly-ɣ-glutamic acid with $^{99m}$Tc. The nanoparticles demonstrate a high affinity for tumor cells that exhibit an overexpression of folate receptors. This specificity enables early detection of tumor through the use of SPECT and SPECT-CT imaging modalities.

In this study, two types of nanoparticles were explored which are chitosan nanoparticles and β-cyclodextrin nanoparticles. Both nanoparticles were characterized and radiolabeled with $^{99m}$Tc. The labelling efficiency and stability of the radiolabeled complex were determined and described.

## 2.3 Chitosan

### 2.3.1 Background

Chitosan is the most well-known derivative of chitin. After cellulose, chitin is the second most abundant natural polysaccharide (Cheung et al., 2015; Kumar, 2000). Chitin has been found in crustacean shells (Pakizeh et al., 2021), insects (Triunfo et al., 2022), in the cell walls of fungi (Fernando et al., 2021; Kulka and Sionkowska, 2023), algae (Rahman and Halfar, 2014), and yeasts (Sun et al., 2018). However, due to its high content and easy processing, the shell of crustaceans such as crabs and shrimps become the major source of chitin for industrial applications (Elieh-Ali-Komi et al., 2016; Pakizeh et al., 2021).

Numerous studies have proved that chitosan has a wide range of applications including as artificial skin (Guerle-Cavero et al., 2021; Vivcharenko et al., 2020), bone regeneration (Tao et al., 2020), dental implants (Alnufaiy et al., 2020), drug delivery (Li et al., 2018; Manjusha et al., 2023), surgical sutures (Altınel et al., 2018), and wound repair (Feng et al., 2021). It is known to have unique properties such as biocompatibility (Mohammed et al., 2017; Tang et al., 2023), biodegradability (Mohammed et al., 2017; Tang et al., 2023), low toxicity (Ezoddini-Ardakani et al., 2012; Mohammed et al., 2017), and antibacterial activity (Tang et al., 2023).

Chitosan is produced through deacetylation of chitin (Figure 2.9). Chitin is a long chain of 2-acetamide-2-deoxy-β-D-glucopyranose (N-acetylglucosamine) units

which are linked by β-(1,4)-glycosidic bonds. Chitin has a carbohydrate backbone with a similar chemical structure to cellulose (Feng et al., 2023). The chemical structures of cellulose, chitin, and chitosan are illustrated in Figure 2.10.

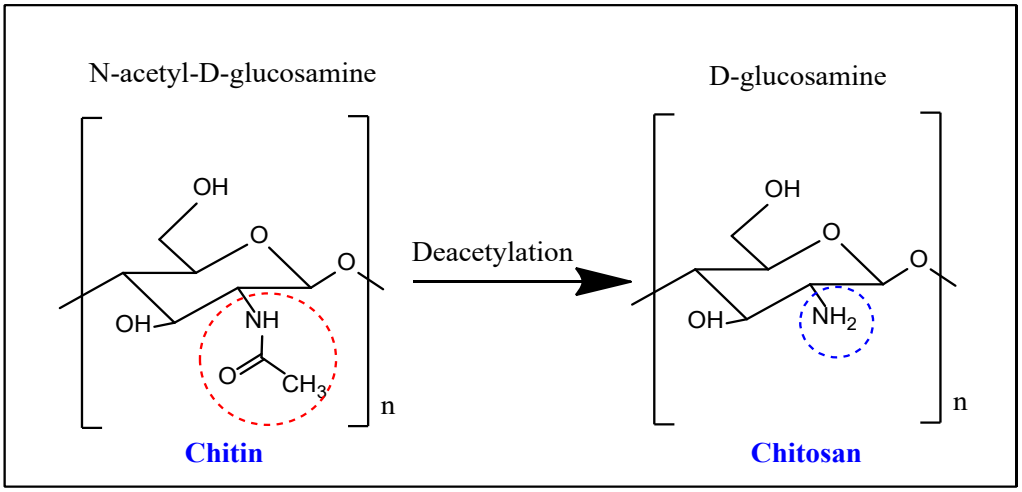


Figure 2.9 Deacetylation of chitin to chitosan